Fluid modeling of anisotropic heating and micro-instabilities in space plasmas

Thierry Passot
UNS, CNRS, Observatoire de la Côte d'Azur, Nice, France

Collaborators:
D. Laveder, L. Marradi, and P.L. Sulem

Dynamics and turbulent transport in plasmas and conducting fluids

Wolfgang Pauli Institute, Vienna
29 march- 1 april 2011

Outline

- The solar wind context
- A novel approach: the FLR Landau fluid model
- 1D driven simulations at quasi-perpendicular angle
    - Heating of ions and electrons as a function of injection scale and beta
    - The case of perpendicular ion heating: constraining effect of the mirror instability
- Conclusions

Statistical study of temperature anisotropies

Turbulence (and/or solar wind expansion) generate temparature anisotropy
This anisotropy is limited by mirror and oblique firehose instabilities.

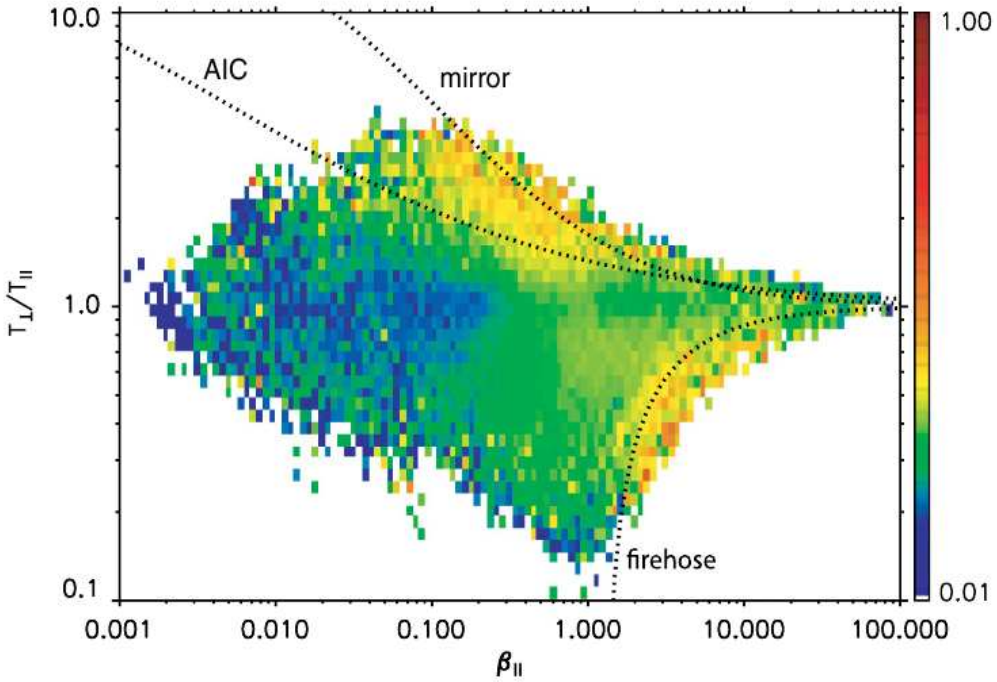

Bale et al. PRL 103, 21101 (2009);
see also Hellinger et al. GRL 33, L09101 (2006).

color: magnitude of δB; enhanced δB also corresponds to enhanced proton heating.

"In a number of systems such as the solar corona and the solar wind, ions are observed to undergo perpendicular heating, despite the fact that most of the fluctuation energy is believed to be in the form of low-frequency kinetic Alfvén wave fluctuations. Determining the cause of such perpendicular heating is one of the critical unsolved problem in the study of space and astrophysical turbulence".

(Report of the Workshop on Research Opportunity in Plasma Astrophysics, Princeton, January 2010)

Non-resonant heating:

Simulation of perpendicular ion heating under the action of given randomly phased KAW with wavelength comparable to the ion Larmor radius on particles for $\beta \lesssim 1$

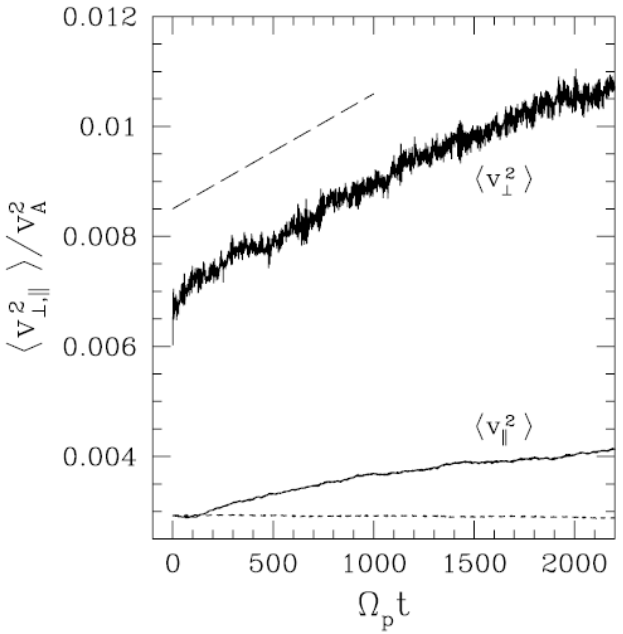

*(Chandran et al. ApJ **720**, 503, 201 see also Bourouaine, 2008)*

Need for a fully nonlinear approach.

Fluid modeling

Goal: describe heliospheric plasmas taking into account

1. collisionless character
2. weak compressibility
3. temperature anisotropy
4. ion and electron Landau damping
5. dispersion due to Hall effet and finite Larmor radius corrections

and possibly
6. electron inertia

Use of the FLR Landau fluid model

Parameters of the 1D simulations:

- Angle of propagation: 80^o with respect to the ambiant magnetic field

- White noise in time random driving around k_{inj}, applied on the perpendicular velocity component (u_y) each time the sum of kinetic and magnetic energy falls below a given threshold: it is intended to simulate the injection of energy from the end of the solar wind Alfvén wave cascade.

Initial temperatures are isotropic with varying parallel proton β.

- The size of the domain L is measured in units of ion inertial length and is varied.

- Number of grid points: typically N=256.

- No dissipation is added.

- Simulations are performed with Ng=512 grid points and desaliased at Ng/2

The simulations are organized in order to:

- Study the heating processes and its dependence on injection scale and β
- Study of generation and saturation of the mirror instability
- Study the influence of collisions
- Briefly address the case where parallel ion temperature dominates

Dependence of heating on beta and injection scale

Fixing $k_{inj}/k_{\rho}=0.087$ (rather small scale) and varying β (thus changing the domain size):

Perpendicular heating and parallel cooling of ions, with a larger efficiency as β is reduced

$T^{i}_{\perp}$

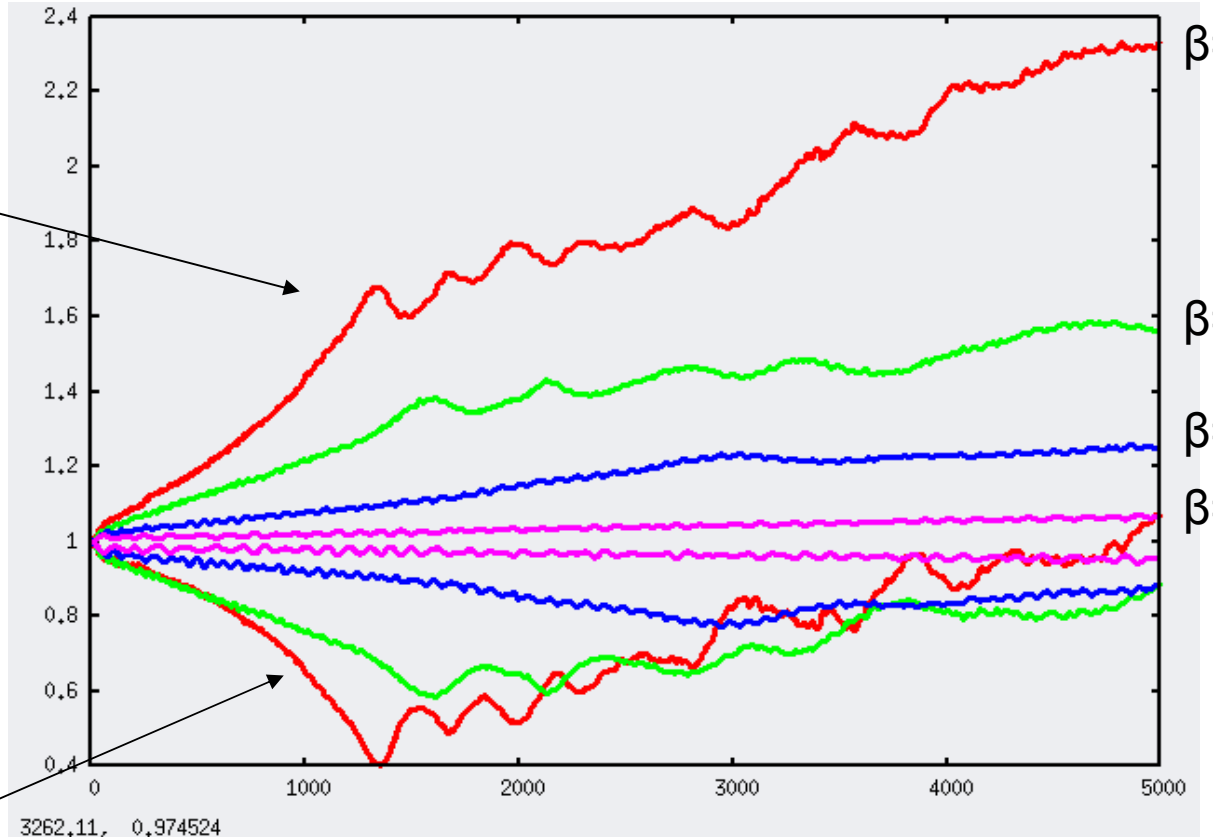

β=0.6

β=1.2

β=2.4

β=9.6

$T^{i}_{//}$

Red: β=0.6, L=12 π
Green: β =1.2, L=16 π
Blue: β =2.4, L=22 π
Pink: β =9.6, L=144 π

Terms leading to temperature variations:

Perpendicular and parallel pressures

$$\begin{cases} \partial_t p_\perp + \nabla\cdot(\vec{u}p_\perp) + p_\perp \nabla\cdot\vec{u} - p_\perp \hat{b}\cdot\nabla\vec{u}\cdot\hat{b} + \dfrac{1}{2}[\mathrm{tr}\,\nabla\cdot\mathbf{q} - \hat{b}\cdot(\nabla\cdot\mathbf{q})\cdot\hat{b}] \\ \quad + \dfrac{1}{2}\left(\mathrm{tr}(\boldsymbol{\Pi}\cdot\nabla\vec{u})^S - (\boldsymbol{\Pi}\cdot\nabla\vec{u})^S{:}\boldsymbol{\tau} + \boldsymbol{\Pi}{:}\dfrac{d\boldsymbol{\tau}}{dt}\right) = 0 \\ \\ \partial_t p_\parallel + \nabla\cdot(up_\parallel) + 2p_\parallel \hat{b}\cdot\nabla u\cdot\hat{b} + \hat{b}\cdot(\nabla\cdot\mathbf{q})\cdot\hat{b} + (\boldsymbol{\Pi}\cdot\nabla\vec{u})^S{:}\boldsymbol{\tau} - \boldsymbol{\Pi}{:}\dfrac{d\boldsymbol{\tau}}{dt} = 0 \end{cases}$$

leading to

$$\begin{aligned} &\frac{dT}{dt} + \frac{2}{3}T(\nabla\cdot u) + \frac{2}{3}(\boldsymbol{\varpi} : \nabla u)\Delta_T \\ &\quad + \frac{3}{n}\,\mathrm{tr}\,(\nabla\cdot\mathbf{q}) + \frac{3}{n}\,\mathrm{tr}\,(\boldsymbol{\Pi}\cdot\nabla u)^s = 0 \\ &\frac{d\Delta_T}{dt} = \Delta_T(\mathbf{I}/3 + \boldsymbol{\tau}) : \nabla u + 3T\boldsymbol{\varpi} : \nabla u + \\ &\quad + \frac{3}{2n}\boldsymbol{\varpi} : \nabla\cdot\mathbf{q} + \frac{3}{2n}\boldsymbol{\varpi} : (\boldsymbol{\Pi}\cdot\nabla u)^s + \frac{3}{2n}\boldsymbol{\Pi} : \frac{d\boldsymbol{\tau}}{dt} \end{aligned}$$

where

$$\begin{cases} T = (2T_\perp + T_\parallel)/3 \\ \boldsymbol{\varpi} = \mathbf{I}/3 - \boldsymbol{\tau} \\ \Delta_T = T_\perp - T_\parallel \end{cases}$$

β=0.6

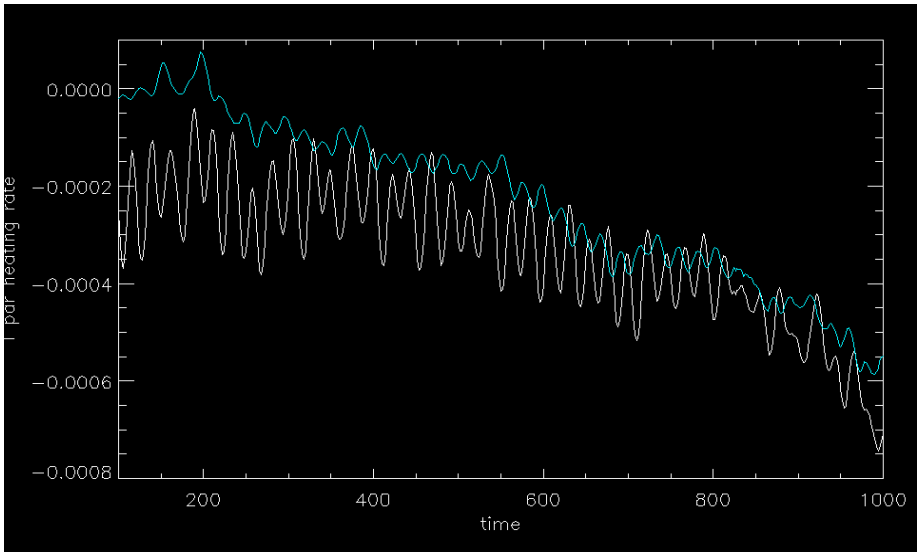

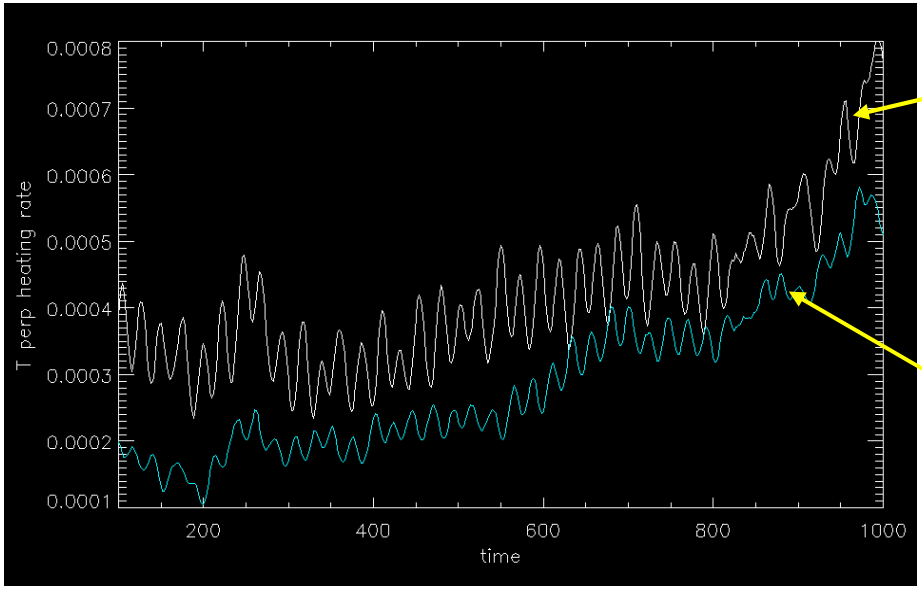

Origin of heating/cooling:

Domination of FLR contribution; more important close to mirror threshold

Parallel cooling

Total temperature variation

Perpendicular heating

FLR contribution

Efficient parallel electron heating at small β

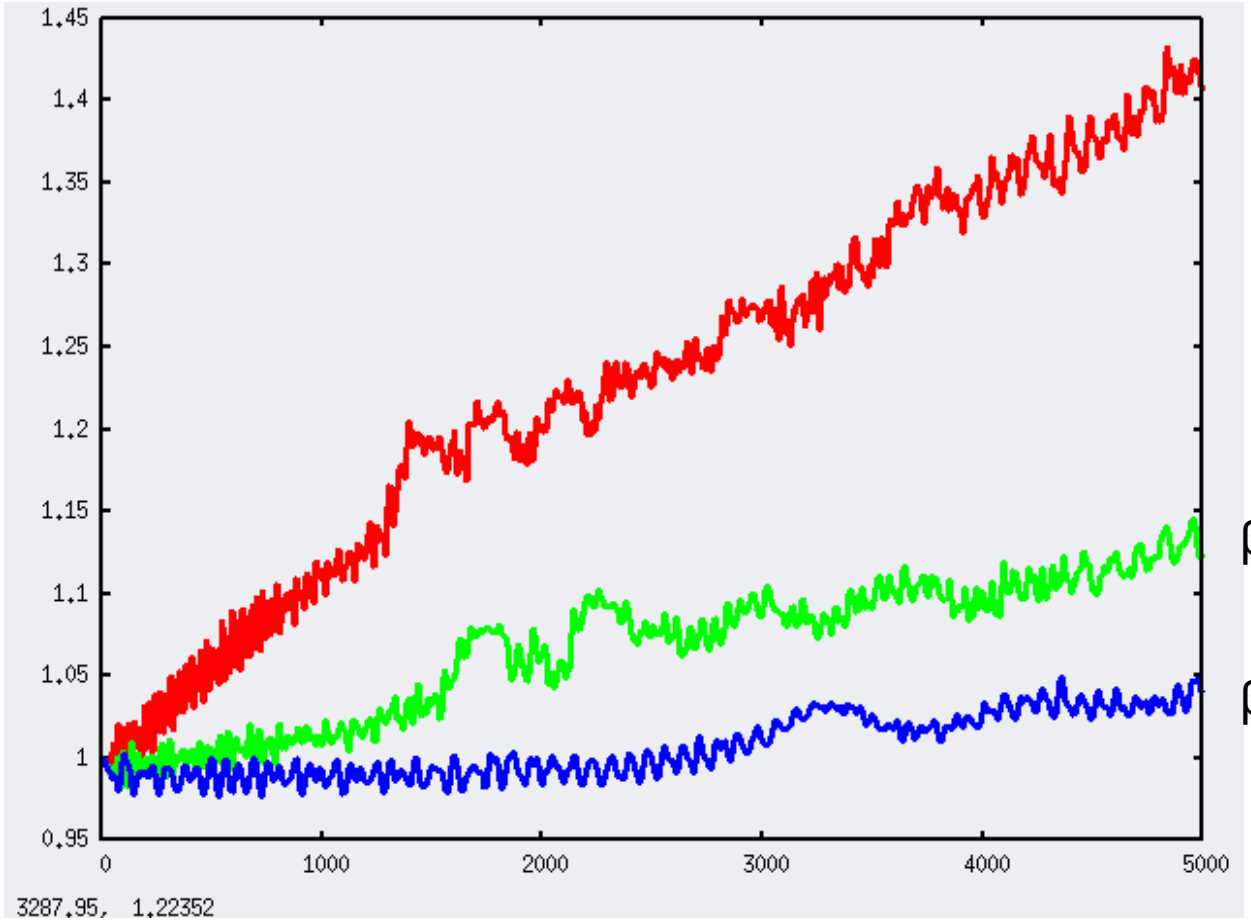

Parallel electron temperature (same conditions)

At a scale k_{inj}/k_ρ=0.062, the behavior is similar.
Frequency analysis for β=0.3

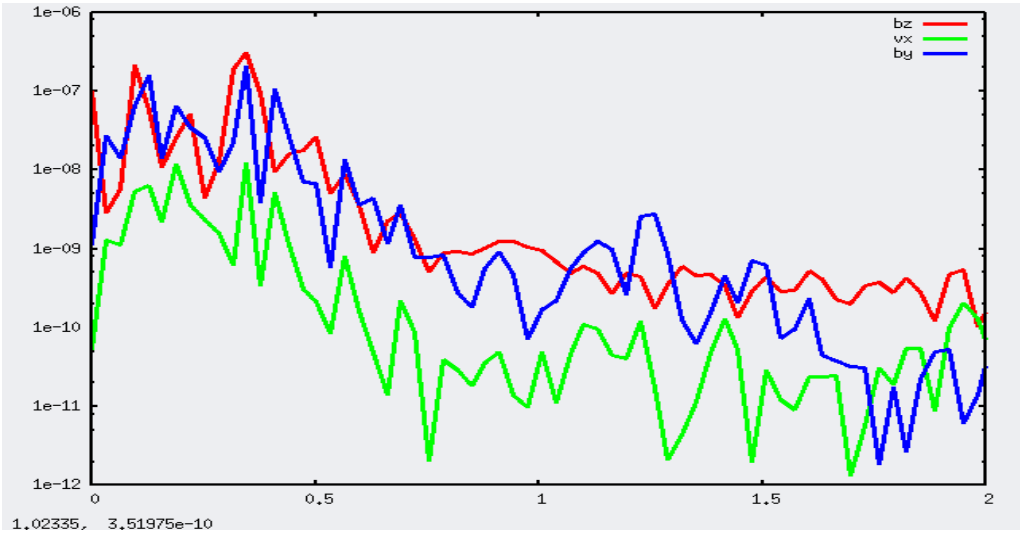

Domination of low-frequency modes (including mirror)

Mode 10
(k_ρ/k=6.4)

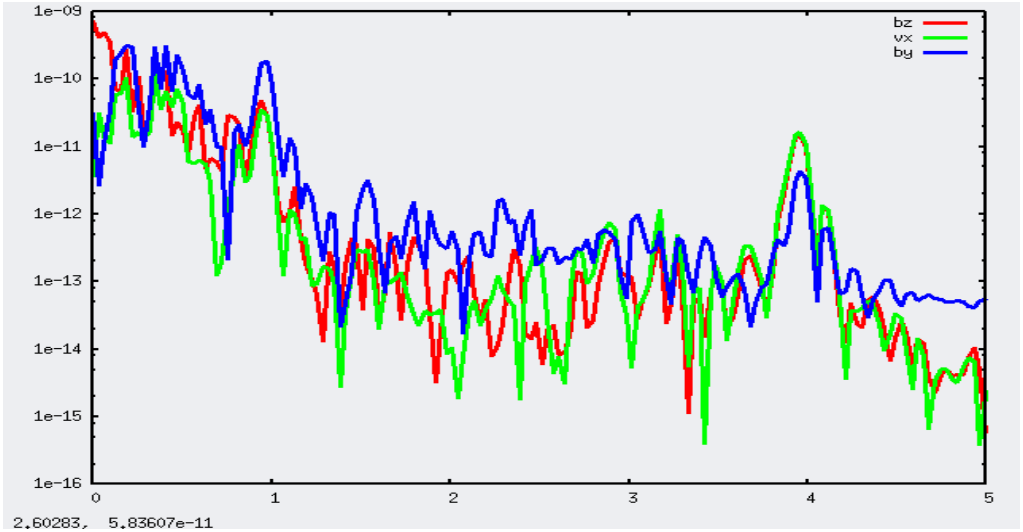

Mode 18
(k_ρ/k=3.6)

Red: b_z
Green: v_x
Blue: b_y

In this regime where the mirror modes are linearly damped, it can be of interest to remark that, in spite of the variety of modes present in the turbulent regime, the temperature evolution derived by the quasi-linear theory (Eqs. (22) and (23) of *Shapiro and Shevchenko* [1964]) leads to, when prescribing a bi-Maxwellian ion distribution function:

$$\frac{dT_{\perp i}}{dt} = -2\Big(\sum_k \gamma_k \frac{|B_k|^2}{B_0}\Big)\Big(1+\frac{2}{\beta_{\perp i}}\Big)T_{\perp i}$$

$$\frac{dT_{\parallel i}}{dt} = 4\Big(\sum_k \gamma_k \frac{|B_k|^2}{B_0}\Big)\Big(1+\frac{2}{\beta_{\perp i}}\Big)T_{\perp i}$$

When the growth rate is negative, the perpendicular temparature increases while the parallel one decreases.

Increasing the injection scale to $k_{inj}/k_{\rho}=0.044$,

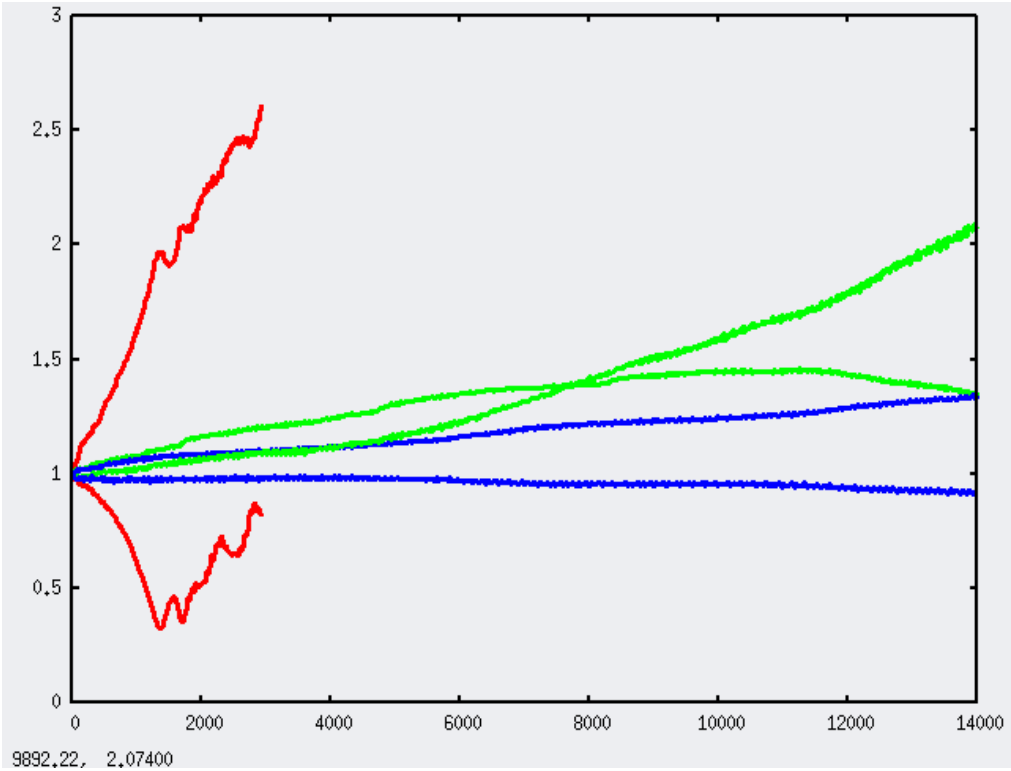

Perpendicular heating keeps being stronger at smaller β in the **initial phase.**

Parallel temperature can end up dominating on longer time at intermediate β

Red: β=0.1
Green: β =0.3
Blue: β =0.6

The initial parallel ion cooling is mainly due to mechanical contributions $T_{//}$ div(u) ($T_{//}$ d/dx (u_x)) associated with magnetosonic waves.

At even larger injection scale to k_{inj}/k_ρ=0.025,

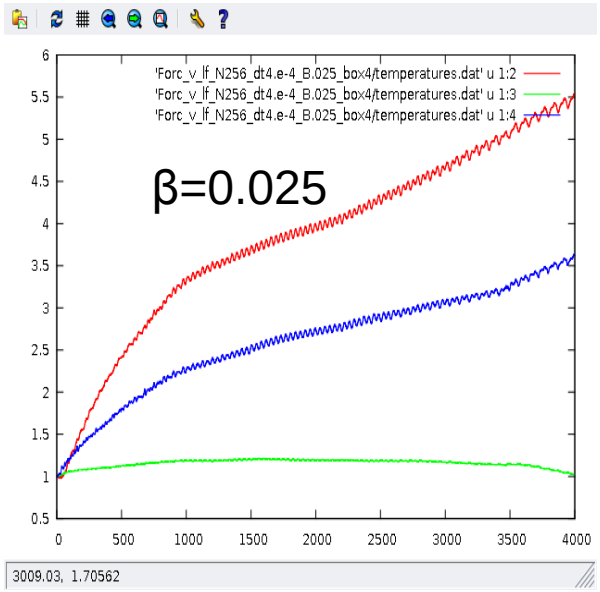

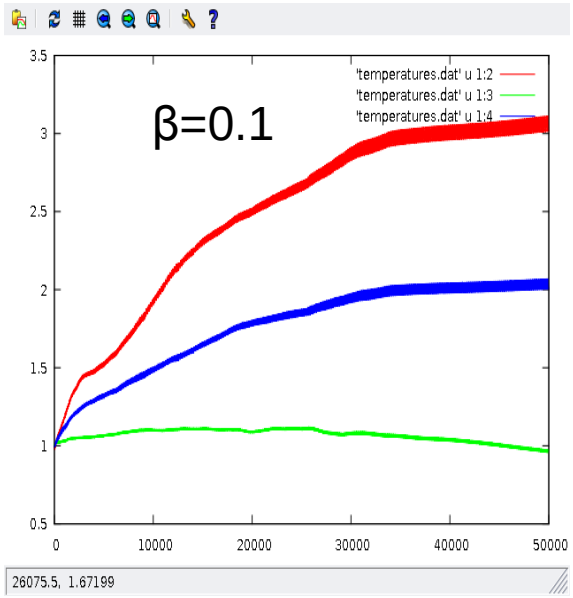

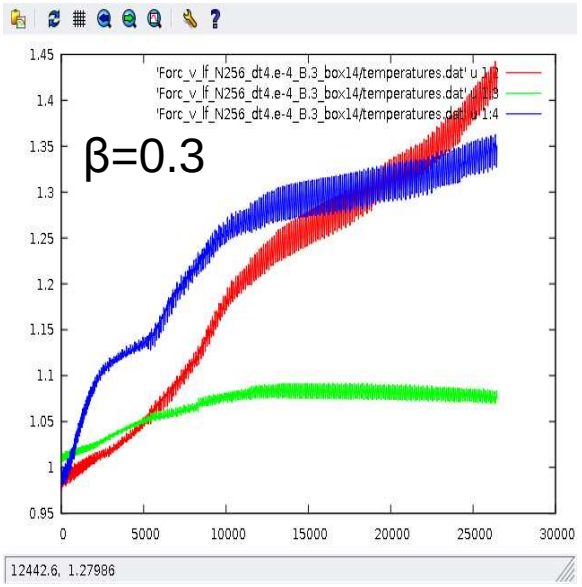

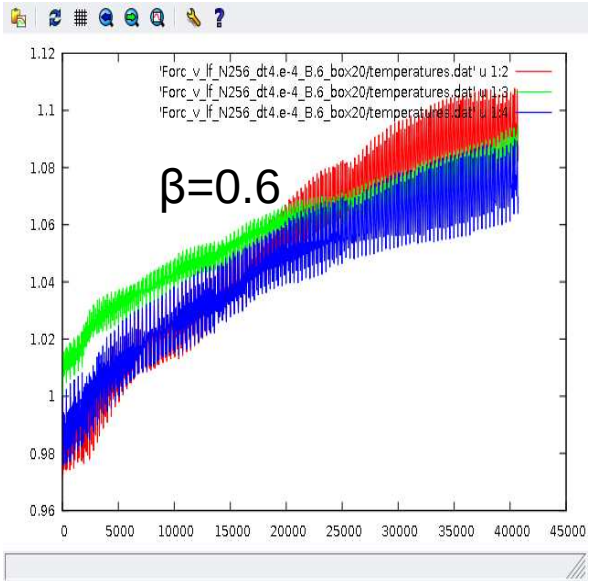

Red: $T^i_{//}$
Green: $T^i_{\perp}$
Blue: $T^e_{//}$

At large injection scale:
There is a critical value of β below which heating affects parallel ion temperature and above which it affects perpendicular ion temperature.

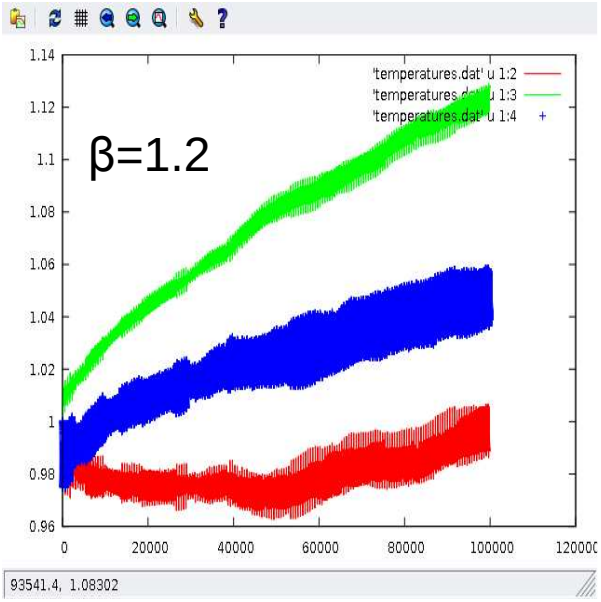

Here k_{inj}/k_ρ=0.022,

Constraining effect of the mirror instability on the growth of temperature anisotropy

Reproduce and understand solar wind temperature anisotropy in WIND data

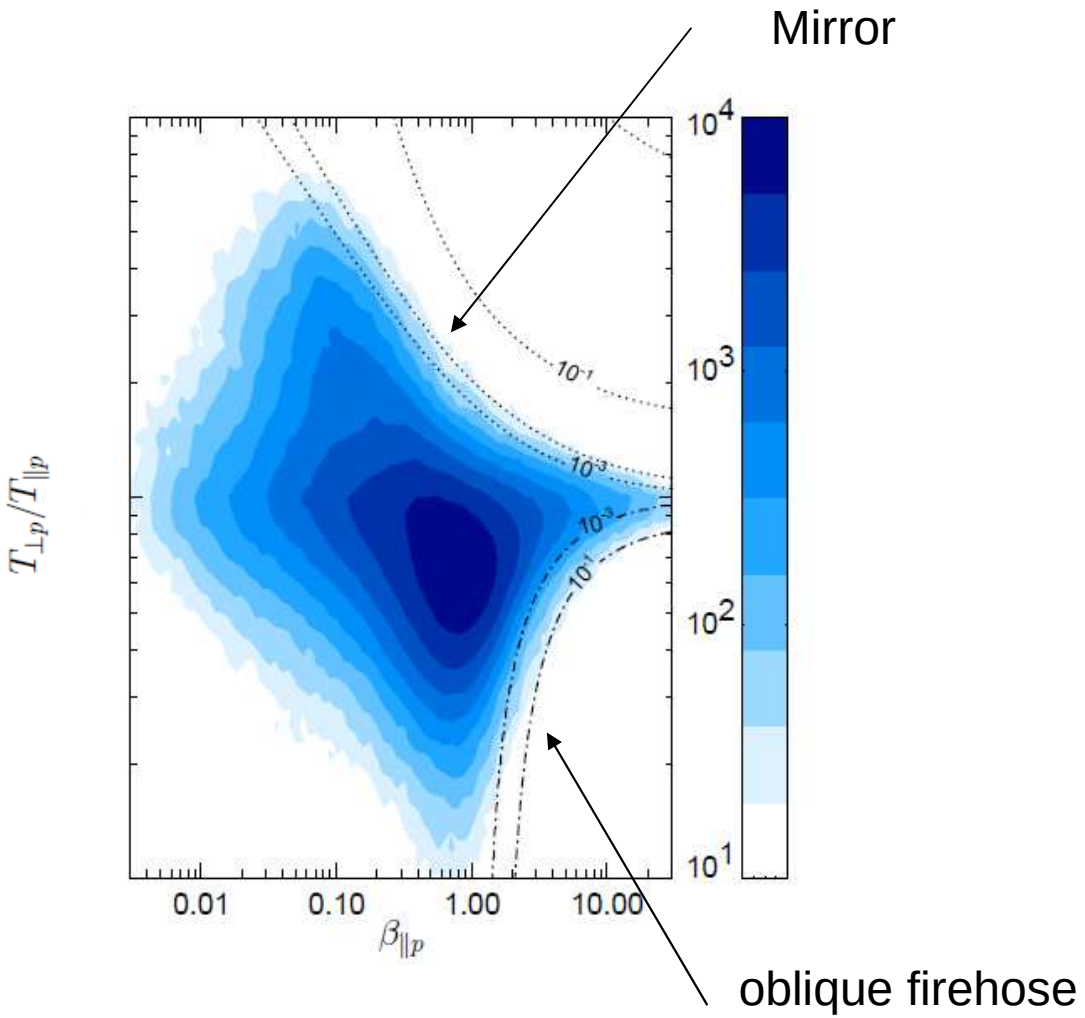

From Hellinger et al. GRL, 33, L09101 (2006)

Global evolution of the mean temperatures

Heating of perpendicular proton temperature
and cooling of parallel proton temperature is
associated with low frequency (damped mirror) modes.
Work of FLR forces is important.

β=0.6

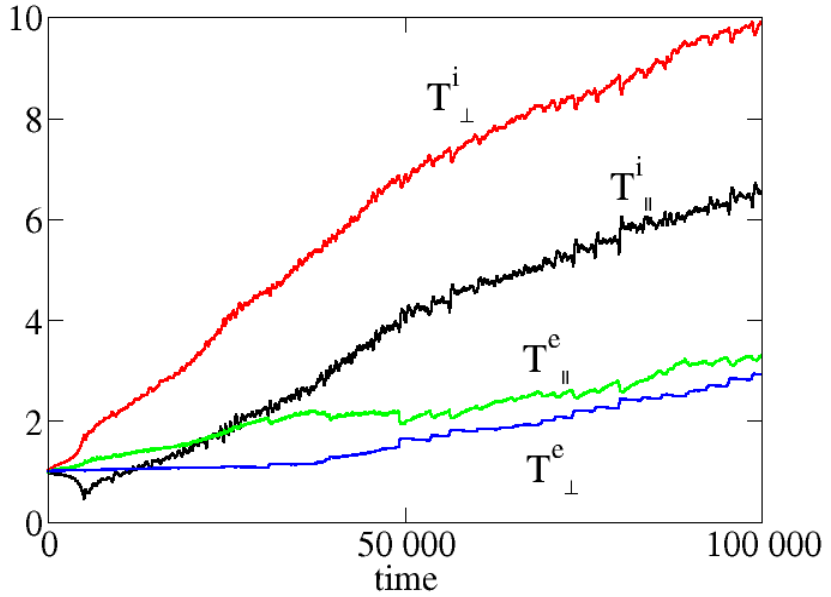

Growth of ion temperatures: $T^i_\perp > T^i_{//}$
More moderate growth of electron temperature: $T^e_\perp < T^e_{//}$

X-T diagram for B_z

Mirror structure

X

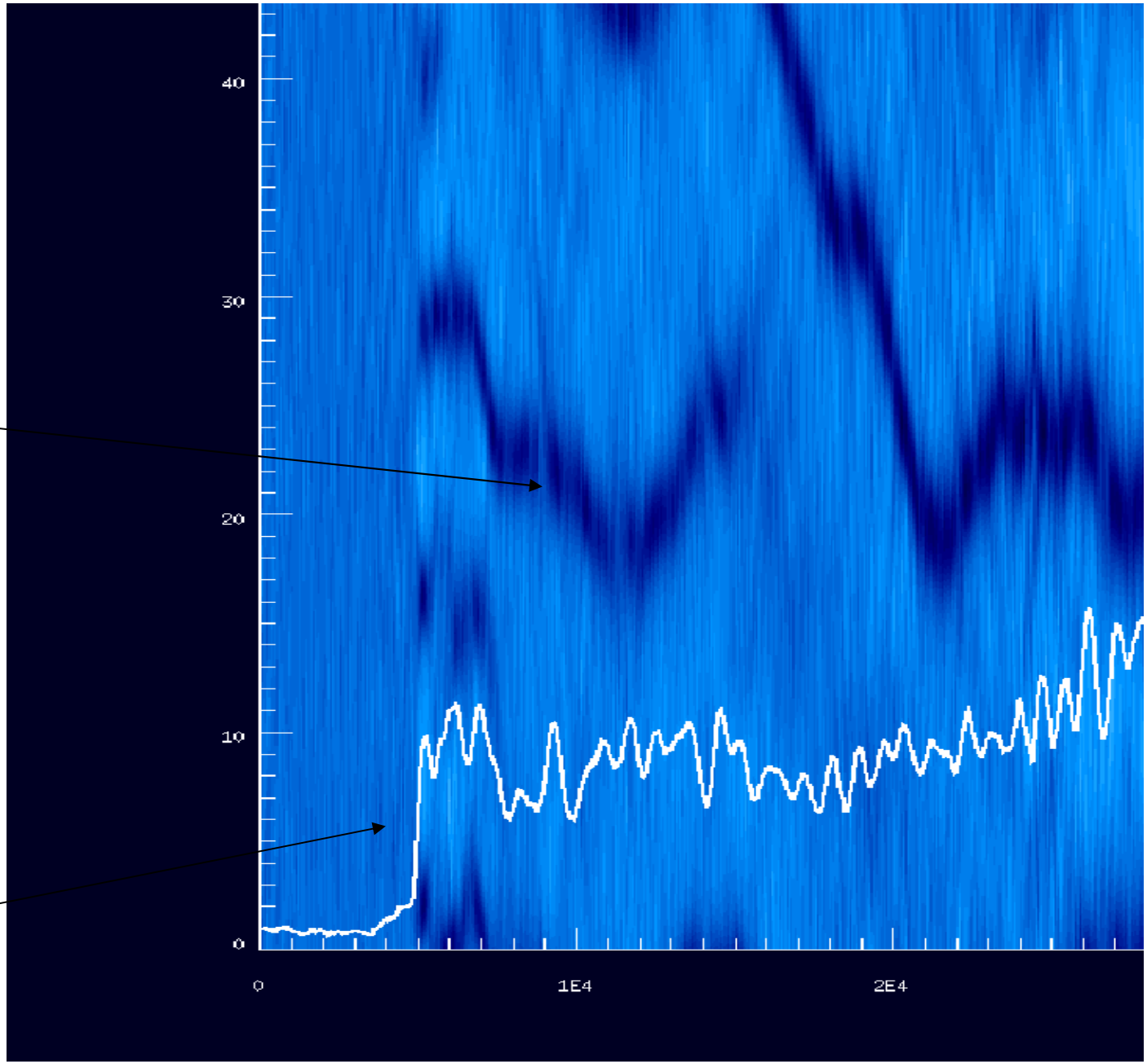

Magnetic compressibility: sharp increase at the onset of the mirror instability

T

Development of the mirror instability

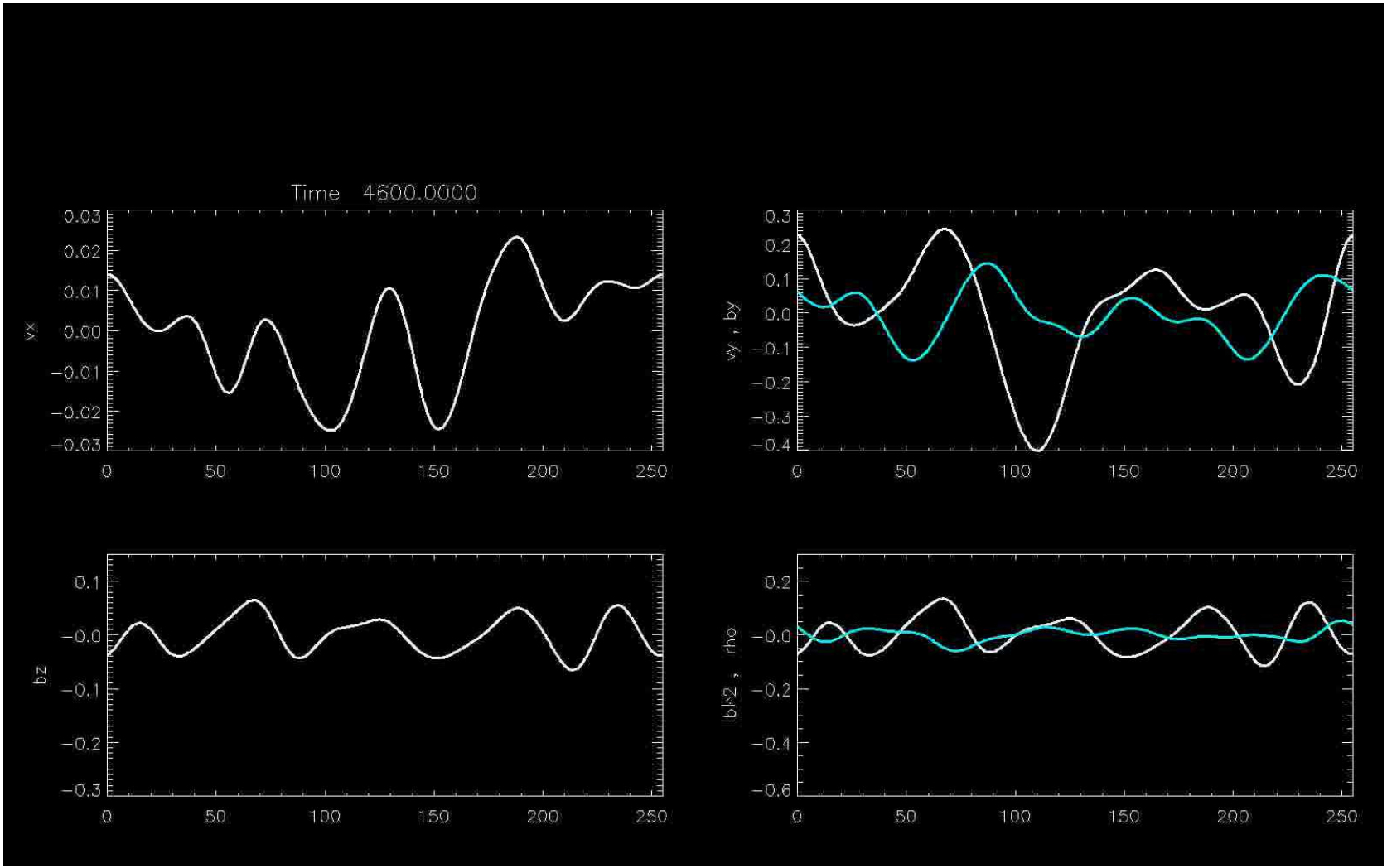

A snapshot just after their formation

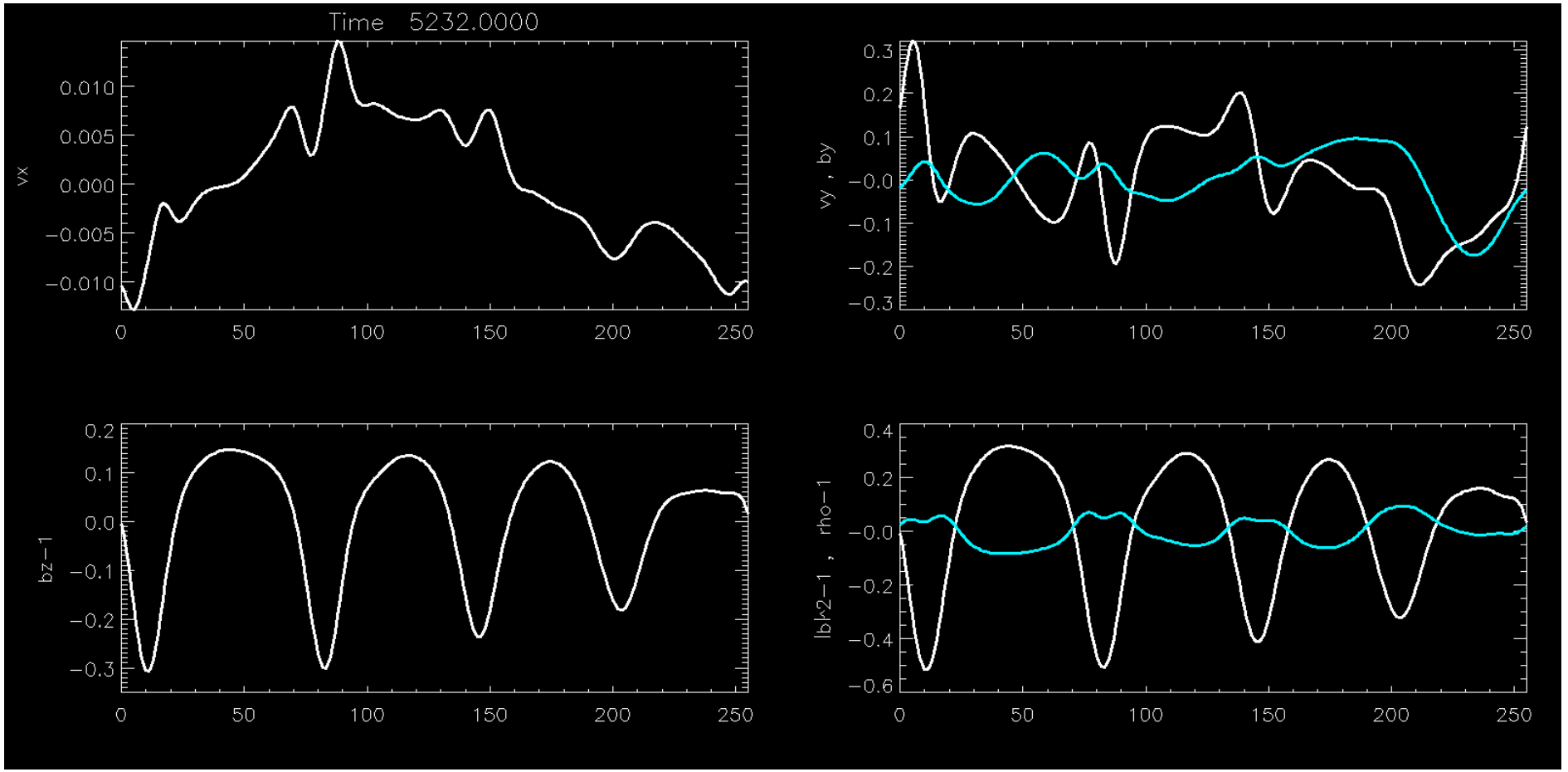

At later times

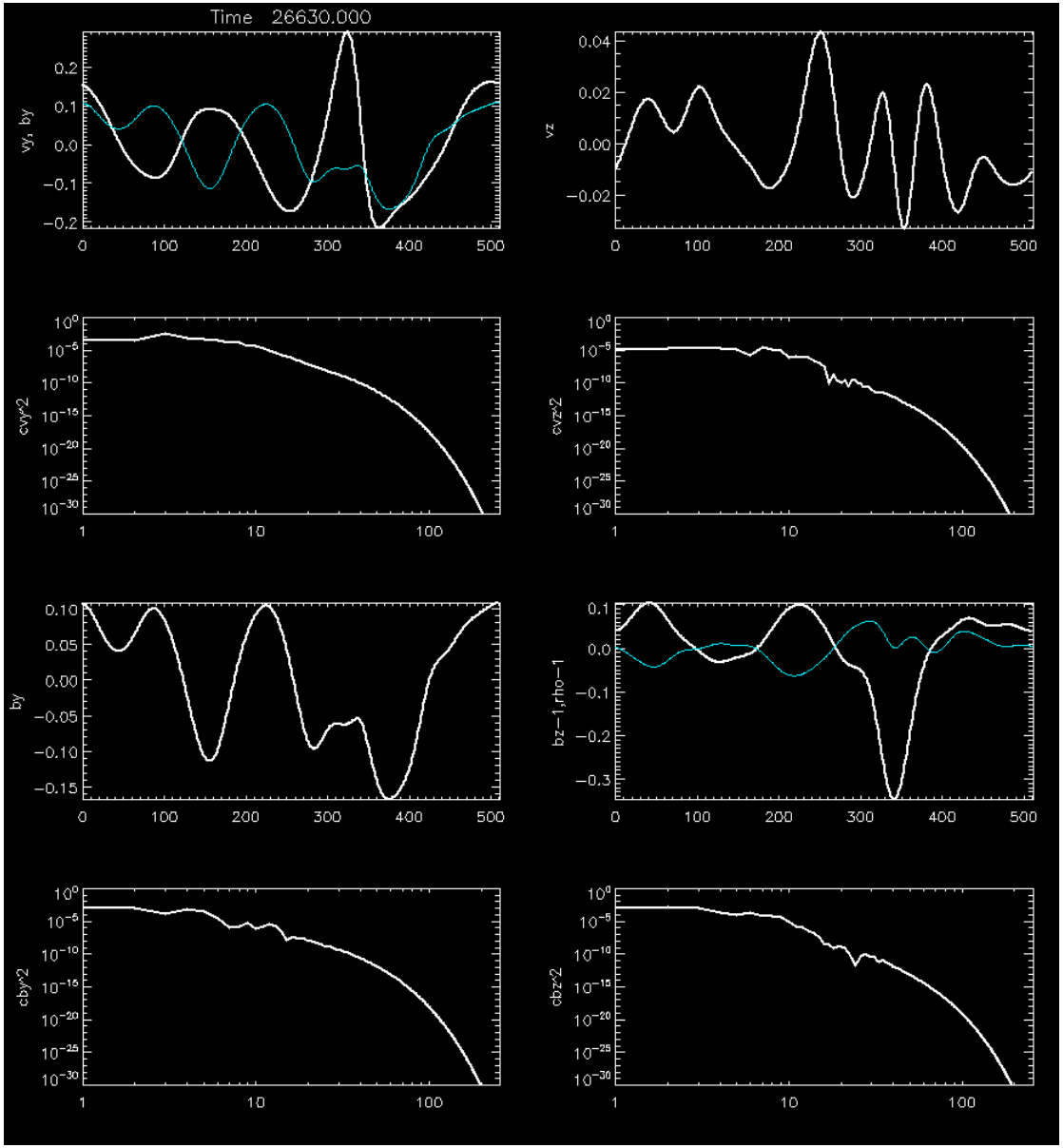

Note the exponential spectra

Apparition of resonances

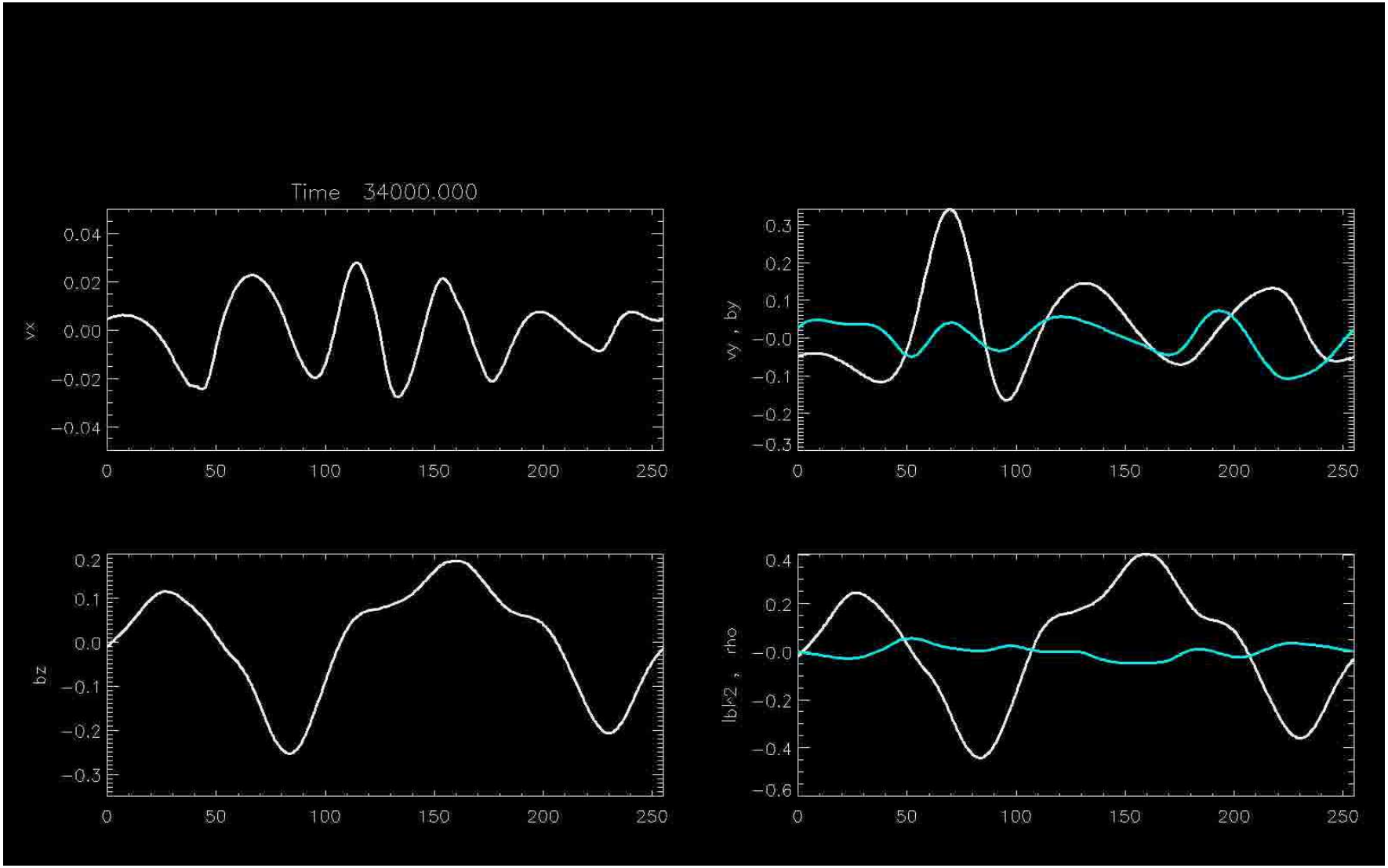

Alfvén resonances due to the inhomogeneity created by the mirror structures.
Leads to power law magnetic energy spectra.

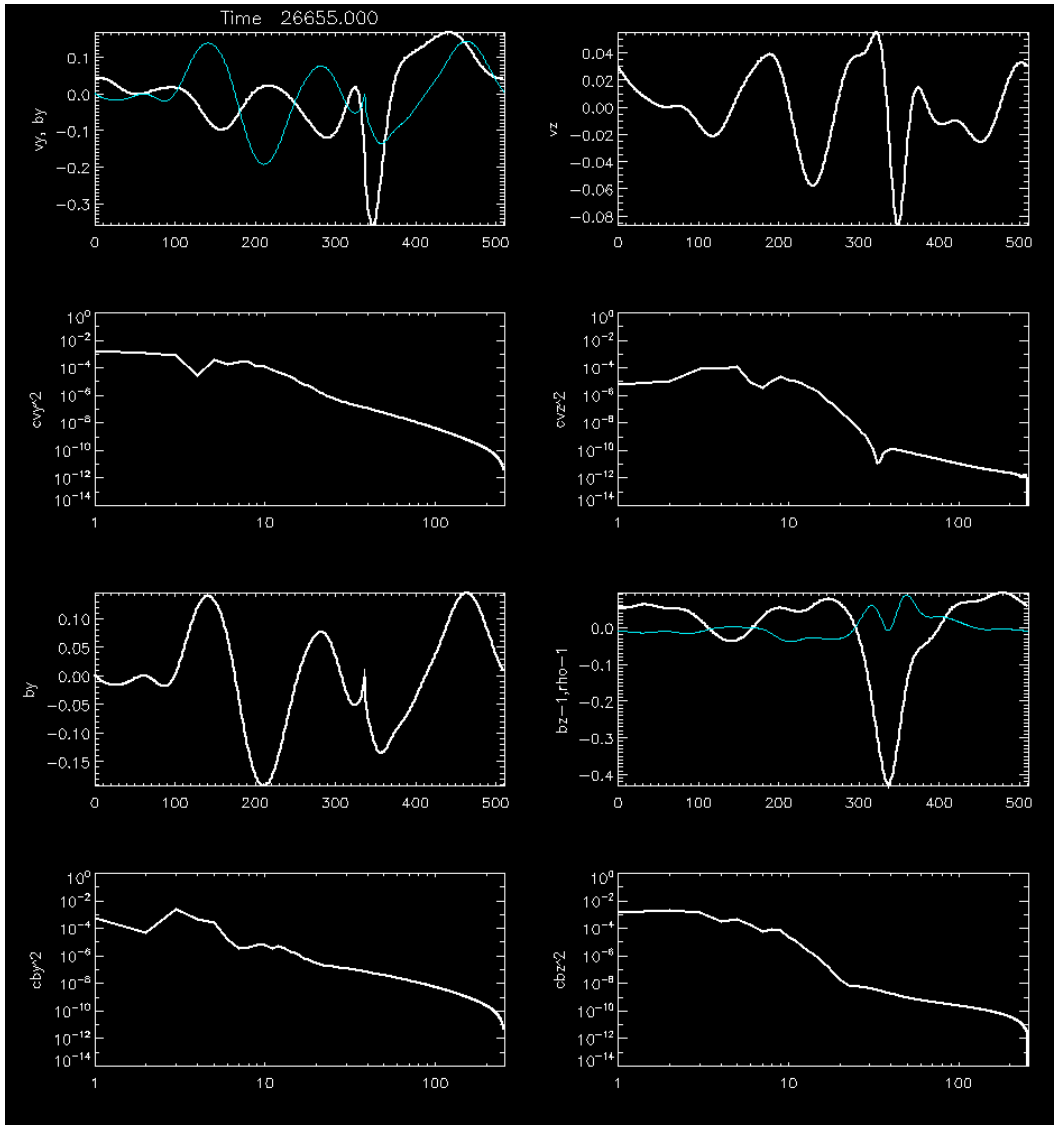

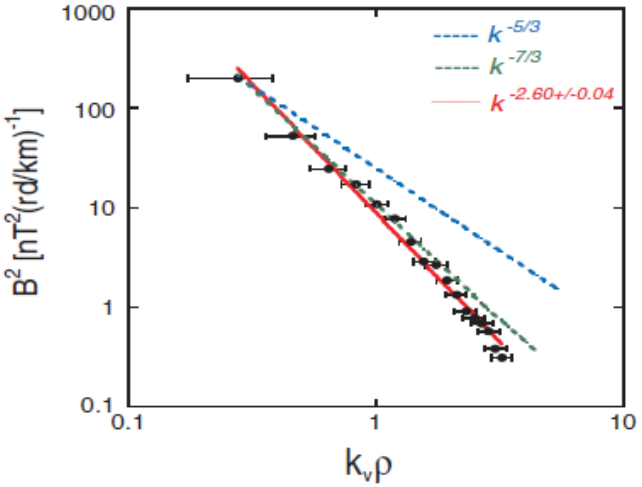

Sahraoui et al. PRL 2006

Distance to mirror threshold

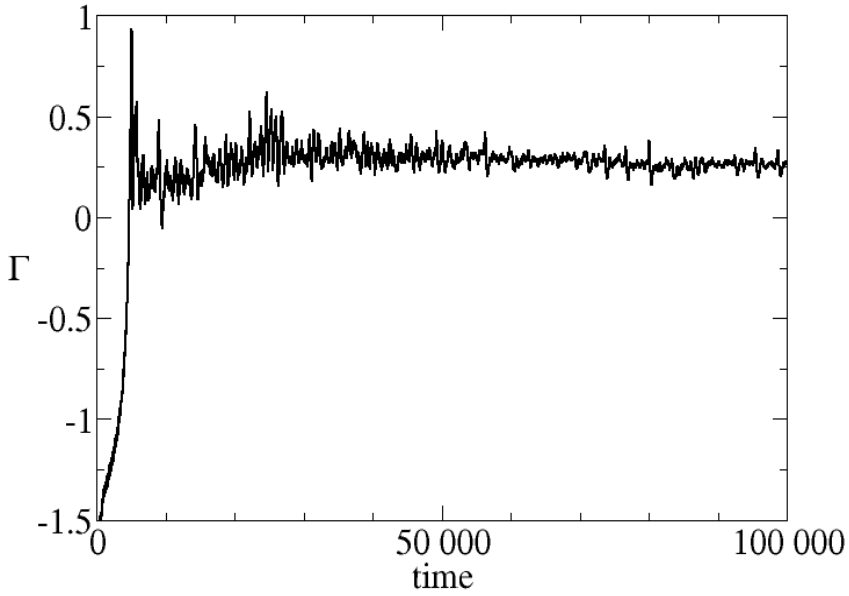

Mirror threshold in presence of hot anisotropic electrons in the long wavelength limit
(Pokhotelov et al. JGR 105, 2393 (2000))

$$\frac{T_{\perp i}}{T_{\parallel i}} - 1 + \frac{T_{\perp e}}{T_{\perp i}}\left(\frac{T_{\perp e}}{T_{\parallel e}} - 1\right) - \frac{T_{\parallel i}T_{\parallel e}}{2T_{\perp i}(T_{\parallel i}+T_{\parallel e})}\left(\frac{T_{\perp i}}{T_{\parallel i}} - \frac{T_{\perp e}}{T_{\parallel e}}\right)^2 - \beta_{\perp i}^{-1} = 0.$$

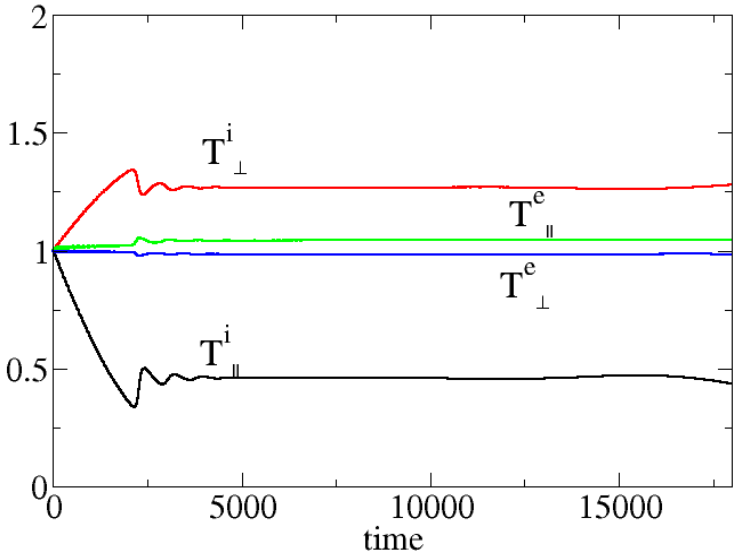

With deterministic forcing on electric field

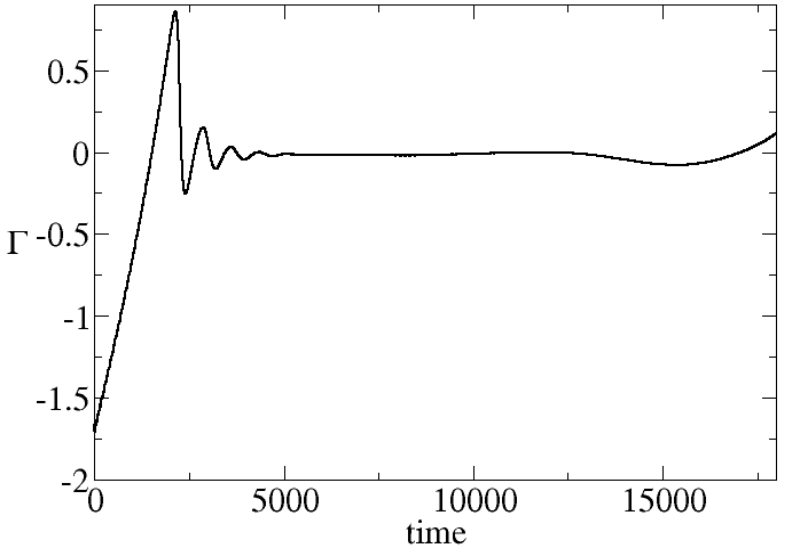

The temperature anisotropy is constrained by the mirror instability

Distance to mirror threshold

$$\Gamma = \beta_{i\perp}\left(\frac{T_{i\perp}}{T_{i\parallel}} - 1\right) + \beta_{e\perp}\left(\frac{T_{e\perp}}{T_{e\parallel}} - 1\right) - 1 - \frac{\left(\frac{T_{i\perp}}{T_{i\parallel}} + \frac{T_{e\perp}}{T_{e\parallel}}\right)^2}{2\left(\frac{1}{\beta_{i\parallel}} + \frac{1}{\beta_{e\parallel}}\right)}$$

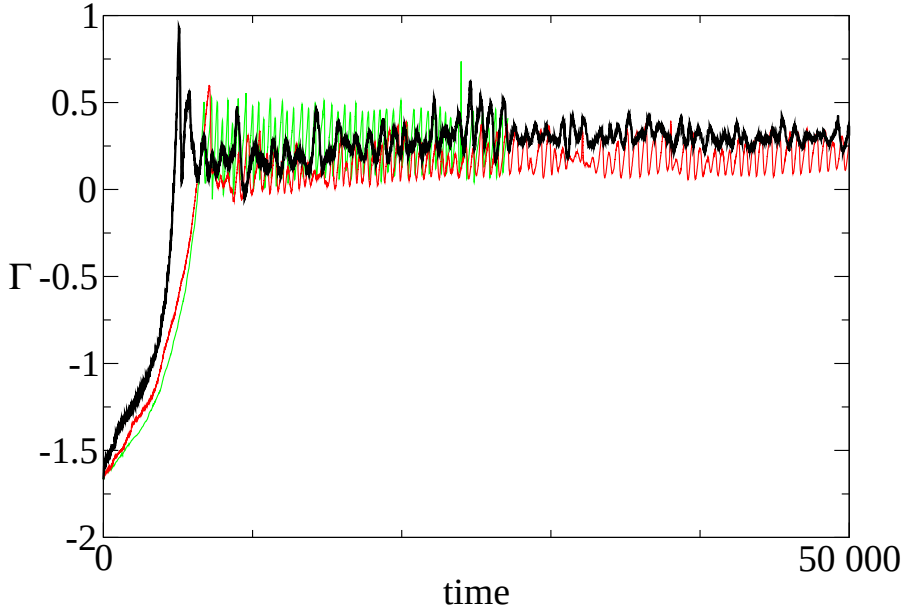

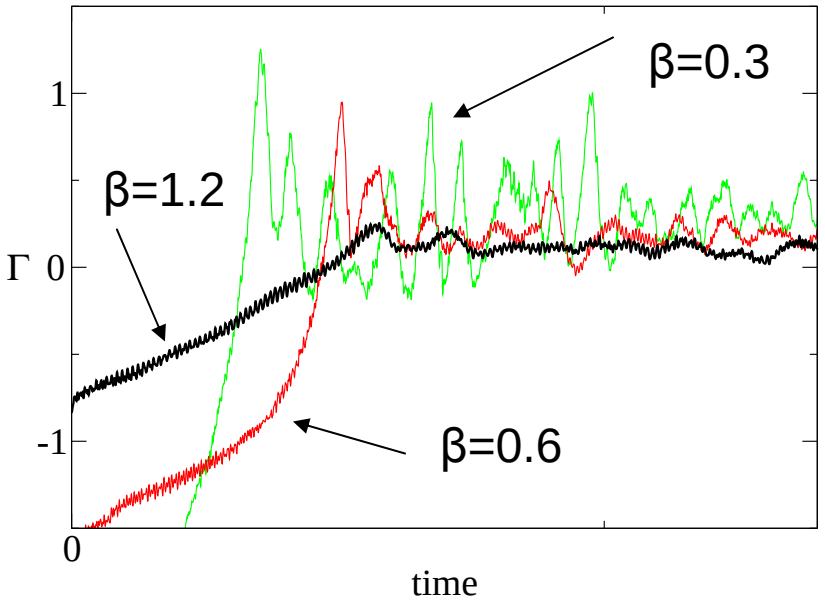

$E_M = \frac{1}{2L}\int(\rho u^2 + b^2)$

0.0159

0.0159 / 4

0.0159 / 16

Influence of the level of kinetic and magnetic energies

Influence of beta, keeping constant $k_{inj}\,\rho_i$

More magnetosonic waves at small beta, leading to a greater distance to threshold

Scatter plot in the beta, temperature anisotropy plane

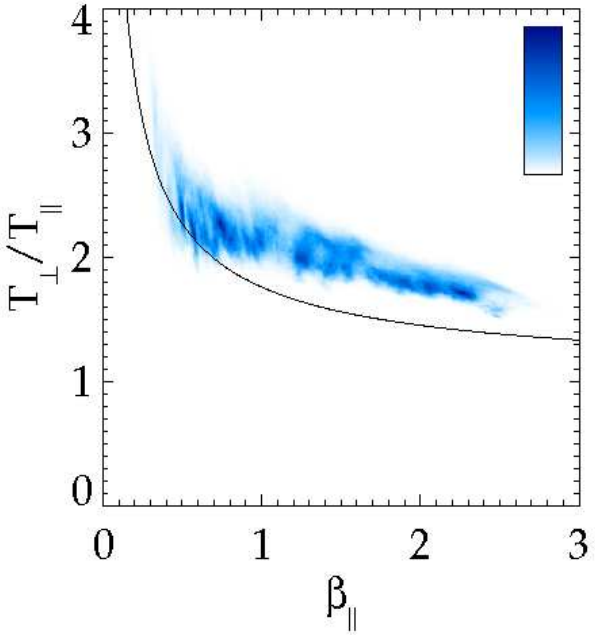

Points: local values of ($\beta_{//}$, $T_\perp / T_{//}$) in the simulation with random forcing at β=0.6

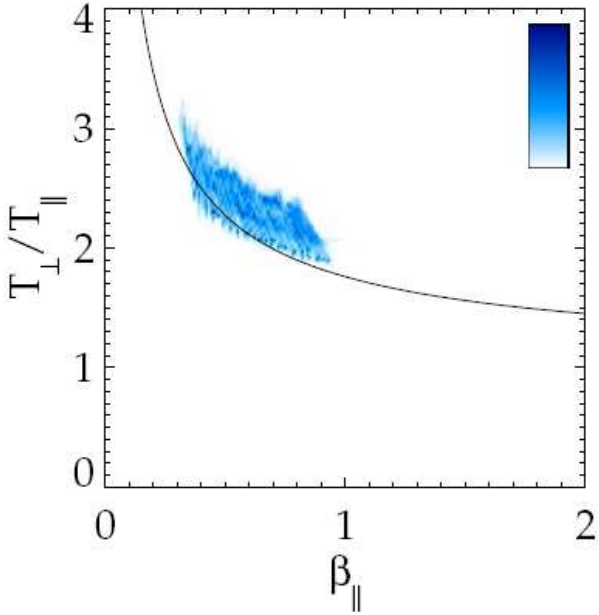

Same, for the simulation with an energy threshold divided by 4

Curve: mirror iso-growth rate at $\gamma=0.001\omega_{ci}$ as given by

$$\frac{T_\perp}{T_\parallel} = 1 + \frac{a}{(\beta_\parallel - \beta_0)^b}.$$

with a=0.77, b=0.76, β_0=-0.016 (Hellinger et al. GRL 2006)

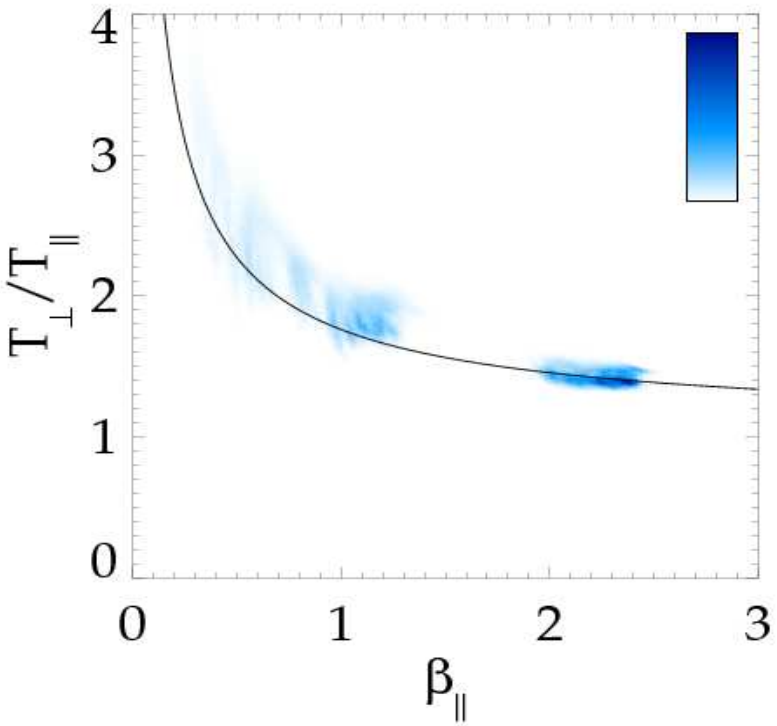

Collecting points from several runs starting at various values of β: the plasma does not enter the unstable range.

Influence of collisions

Introduction of weak collisions

The (too) simple form of Krook collision operator is adopted.

$$\partial_t f_s + \mathbf{v}\cdot\nabla f_s + \frac{q_s}{m_s}\left(\mathbf{E} + \frac{\mathbf{v}}{c}\times\mathbf{B}\right)\cdot\nabla f_s = C(f_s)$$

$$C(f_j) = -\sum_k \nu_{jk}(f_j - F_{Mjk}) \quad \text{with,}$$

$$F_{Mkj} = \frac{n_k}{\pi^{3/2} v_{th,k}^3} e^{-\frac{(v_z-u_{z,j})^2}{v_{th,k}^2}} e^{-\frac{(v_y-u_{y,j})^2}{v_{th,k}^2}} e^{-\frac{(v_x-u_{x,j})^2}{v_{th,k}^2}}$$

$$V_{th,k} = \left(\frac{2T_k}{m_k}\right)^{1/2}$$

$$T_k = \left(\frac{T_\parallel + 2T_\perp}{3}\right)$$

$$\nu_{ii} = \nu_{ee}\left(\frac{m_e}{m_i}\right)^{\frac{1}{2}}$$

$$\nu_{ie} = \nu_{ee}\left(\frac{m_e}{m_i}\right)$$

$$\nu_s = \nu_{ii} + \nu_{ie}$$

Deriving the Landau fluid model with collisions leads to:

r.h.s. of pressure equation

$$C_{\perp r} = \frac{1}{3}(\nu_{rr} + \nu_{r\bar{r}})\frac{\rho}{\rho_0}(p_{\parallel r} - p_{\perp r}) + \frac{1}{2}\frac{m_i \nu_{ie}}{n_0 e^2}[j^2 - (j \cdot \widehat{b})^2]$$

(8)

$$C_{\parallel r} = -\frac{2}{3}(\nu_{rr} + \nu_{r\bar{r}})\frac{\rho}{\rho_0}(p_{\parallel r} - p_{\perp r}) + \frac{m_i \nu_{ie}}{n_0 e^2}(j \cdot \widehat{b})^2 \qquad (9)$$

r.h.s. of heat flux equation

$$Q_{\parallel r} = -(\nu_{rr} + \nu_{r\bar{r}})\frac{\rho}{\rho_0} q_{\parallel r} \mp \nu_{r\bar{r}}(p_{\parallel r} + 2p_{\perp r})\frac{j \cdot \widehat{b}}{e n_0}$$

$$\mp \nu_{ie}\frac{m_i^2}{e^3 n_0}\frac{1}{\rho}(j \cdot \widehat{b})^3 \qquad (10)$$

$$Q_{\perp r} = -(\nu_{rr} + \nu_{r\bar{r}})\frac{\rho}{\rho_0} q_{\perp r} \mp \frac{1}{3}\nu_{r\bar{r}}(p_{\parallel r} + 2p_{\perp r})\frac{j \cdot \widehat{b}}{e n_0}$$

$$\mp \frac{1}{2}\nu_{ie}\frac{m_i^2}{e^3 n_0}\frac{1}{\rho}[j^2 - (j \cdot \widehat{b})^2](j \cdot \widehat{b}). \qquad (11)$$

with, in addition, the Joule term in the magnetic field equation and a linear term in the fourth order cumulant equation $r_{//\perp}$

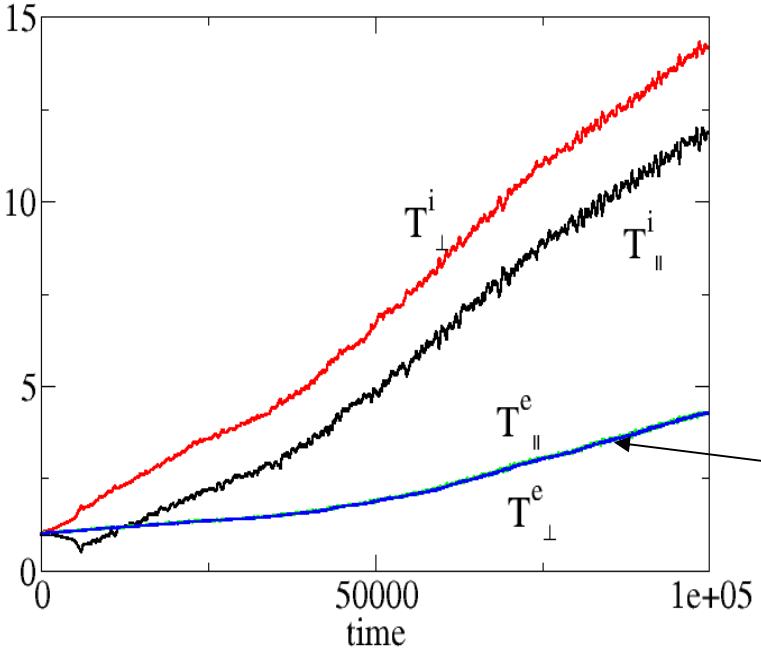

With a small amount of collisions

Equal parallel and perpendicular electrons temperatures.

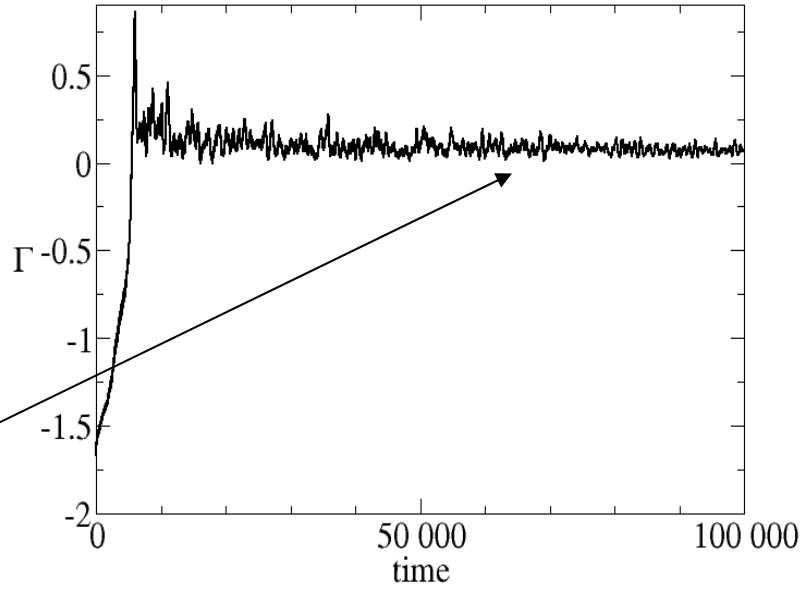

Closer distance to threshold.

With collisions the points lie below the threshold curve but follow it for a very large range of values of the collision frequency.

The cloud lies around $T_\perp / T_{//} = 1$ only for very strong collisions

Weak collisions

$\nu_{ee} = 6.25 \times 10^{-7}$

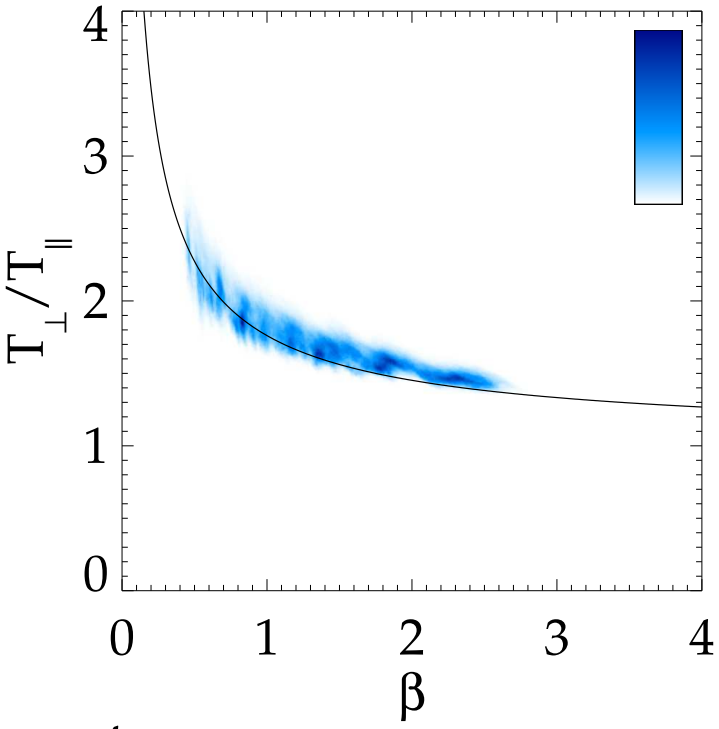

Stronger collisions

$\nu_{ee} = 2.5 \times 10^{-6}$

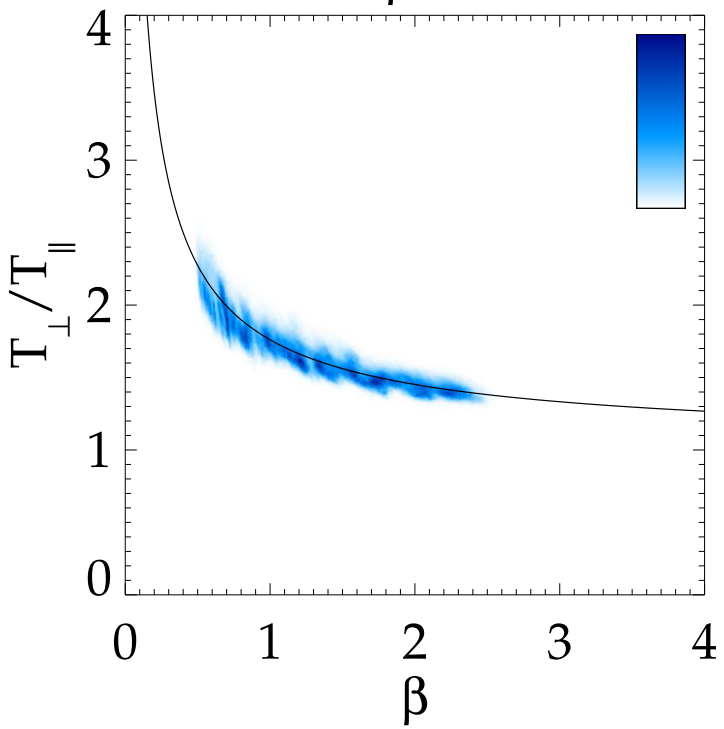

Over a wider β range

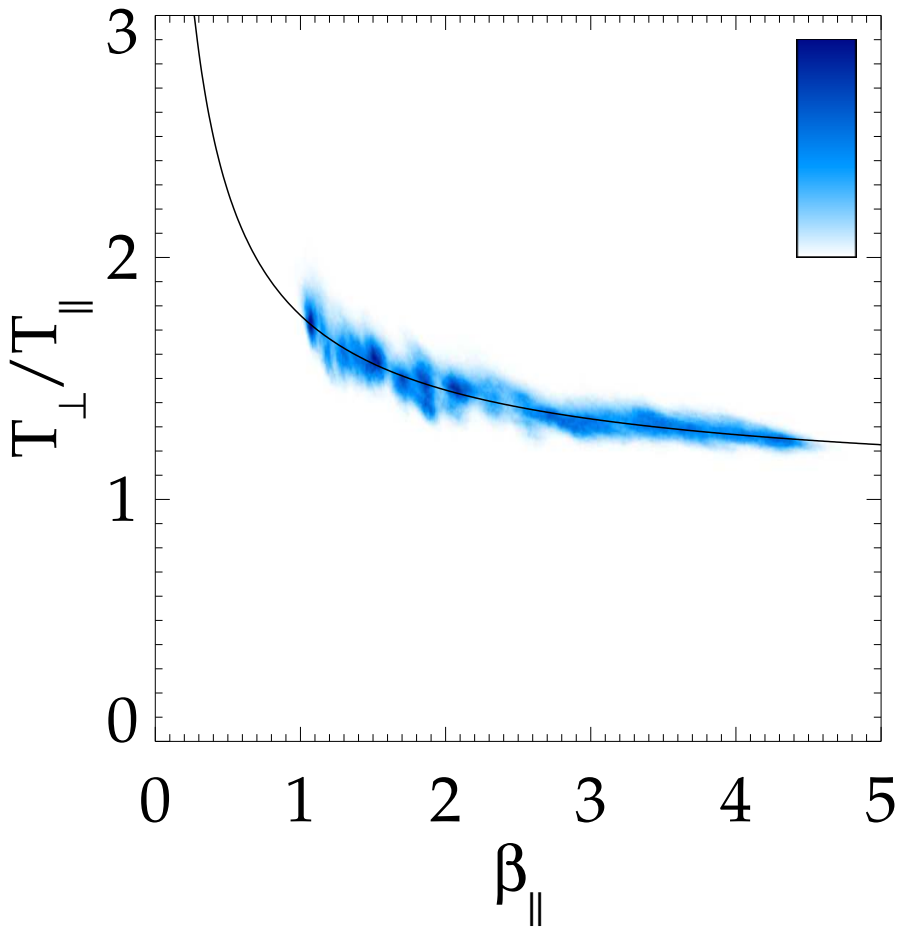

Case where the forcing is applied on the parallel magnetic field B_z

Peak of magnetosonic wave intensity

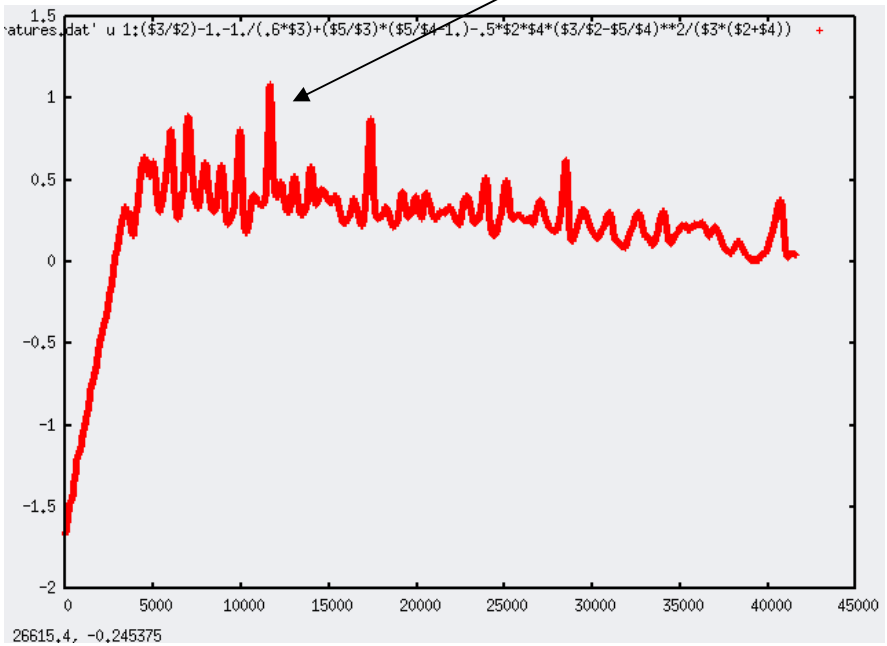

ρ-1

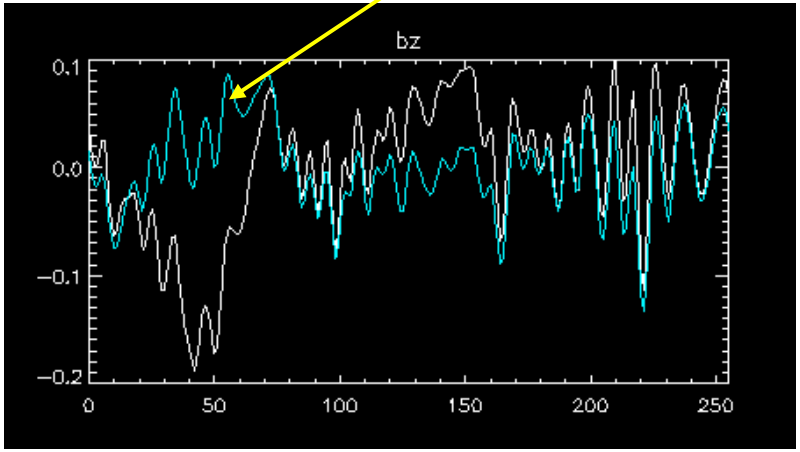

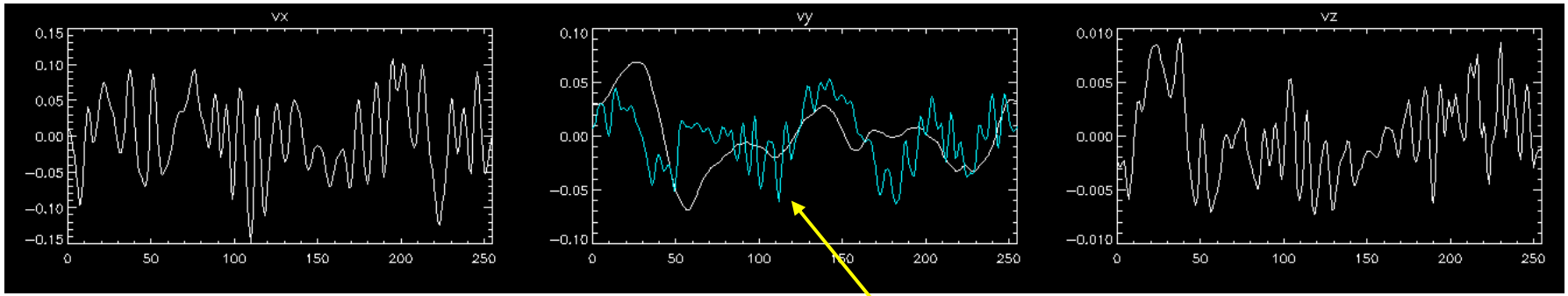

b_y

Magnetosonic solitons

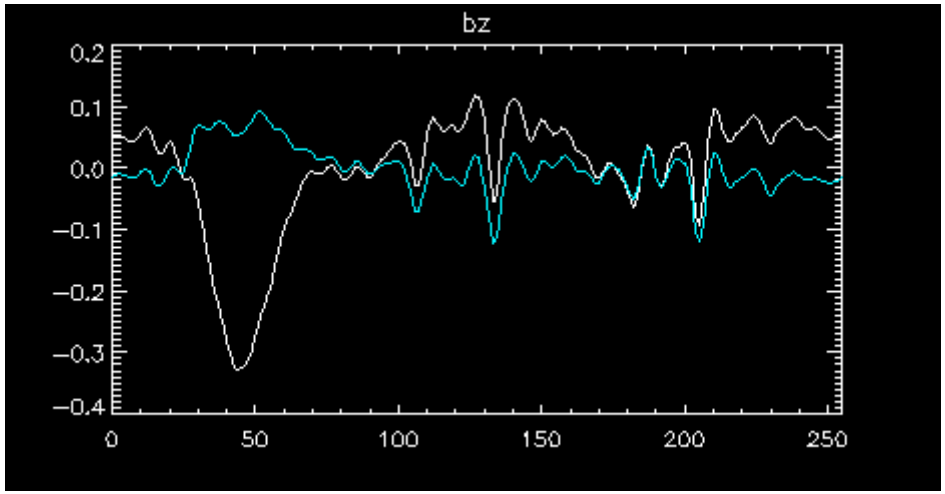

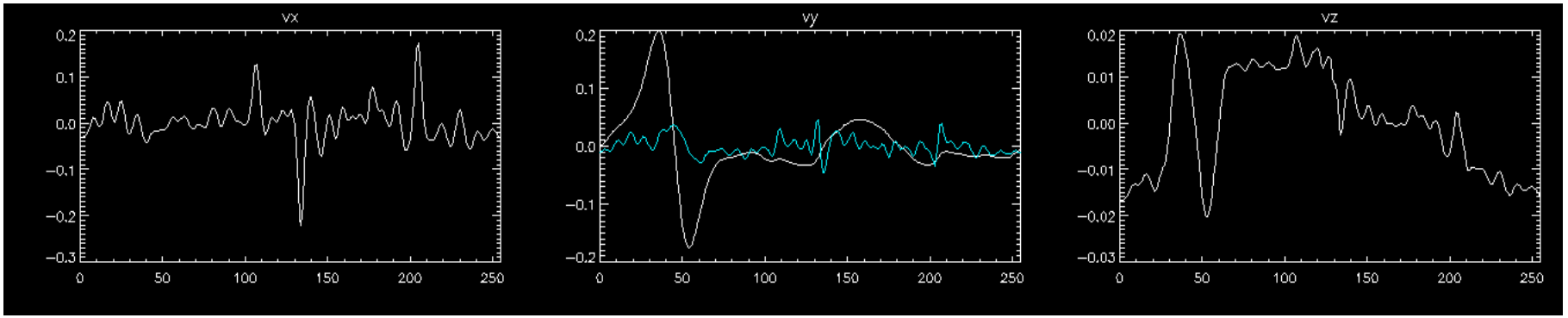

Saturation of the growth of parallel ion temperature

Parallel ion heating and formation of Alfvenic solitons

Forcing on b_y, β=0.6, k_{inj}/k_ρ= 0.062, smaller energy threshold

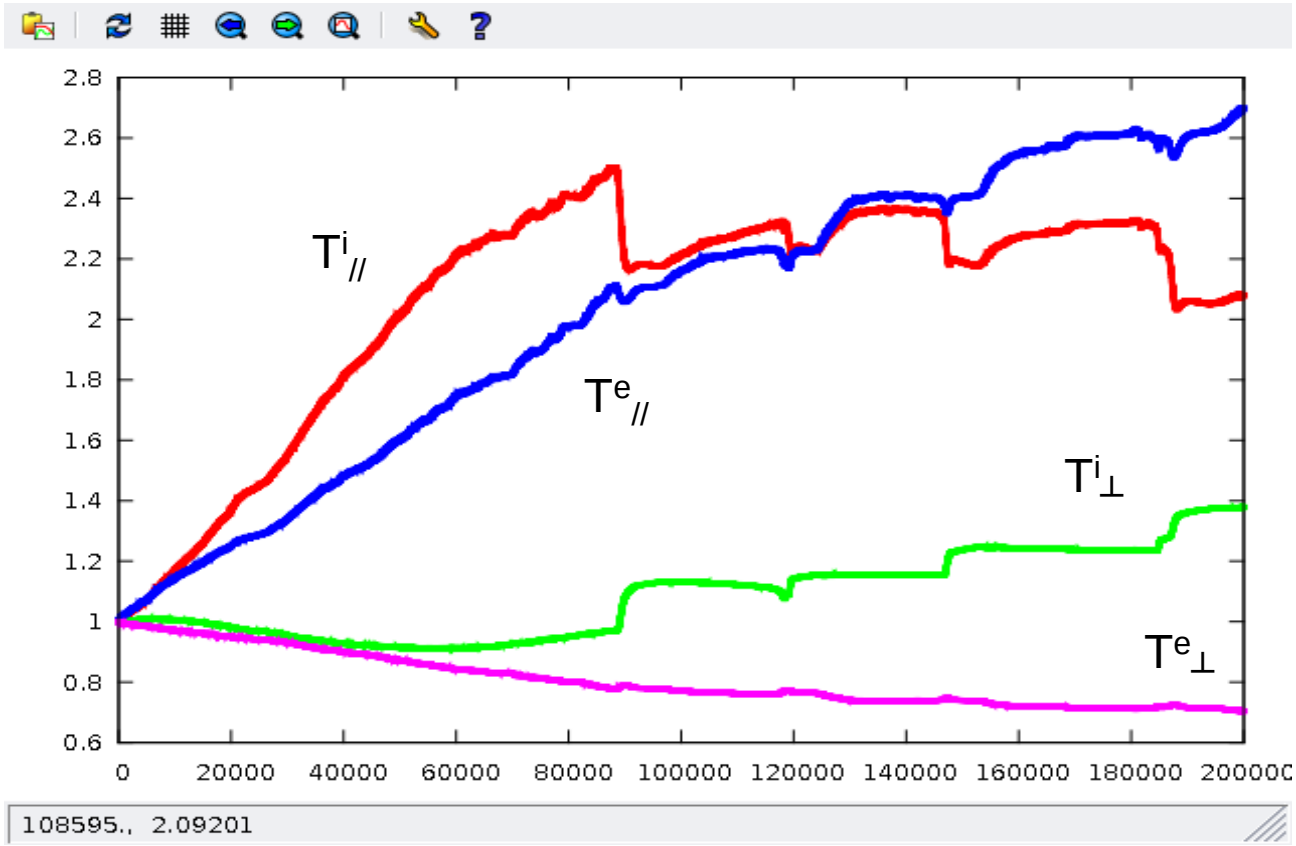

Alfvénic soliton

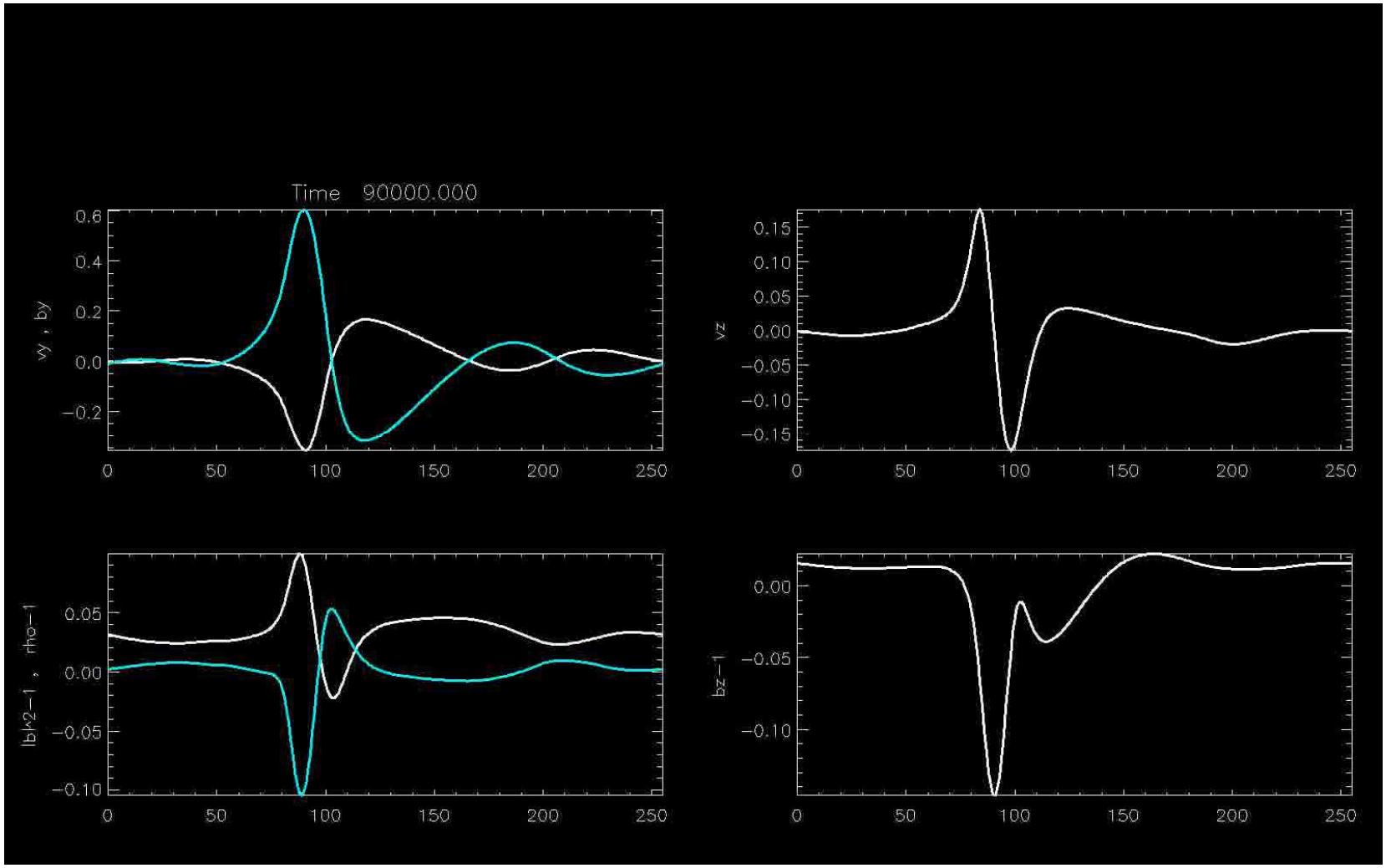

Conclusions

The FLR Landau fluid model allows for the study of heating due to wave turbulence with typical scale close to the ion Larmor radius.

In particular it permits a self-consistent approach.

Simulations are possible without addition of artificial dissipation.

Main results :

- Perpendicular ion heating is possible in nonresonant situations, with KAW driving, when turbulence typical scales are close to the ion gyroradius.
- At constant injection scale, its efficiency increases as β decreases.
- With larger injection scale, heating is very weak and can affect preferentially the ion parallel temperature (as well as the parallel electron temperature) at small values of β
- A diagram of plasma state in ($\beta_{//}$, $T_{\perp}/T_{//}$) plane similar to the one observed in the solar wind is obtained.
- A weak level of collisions helps to constrain the plasma close to the mirror instability threshold.